FM PROCESSING WITH GENERALIZED AMPLITUDE & PHASE: APPLICATION TO MODULATION DOMAIN GEOMETRIC IMAGE TRANSFORMATIONS

Chuong T. Nguyen[†], *Jonathan D. Williams*[†], *Joseph P. Havlicek*[†], *and Murad Özaydın*[‡]

[†]School of Electrical and Computer Engineering, [‡]Department of Mathematics
University of Oklahoma, Norman, OK 73019 USA

ABSTRACT

We introduce new generalized AM and FM functions to perform nonlinear image filtering in the modulation domain with consistent, artifact free phase reconstruction. The new framework enables us to design nonlinear filters in the modulation domain that are capable of producing perceptually motivated signal processing results. As an illustration, we demonstrate that the modulation domain geometric image transformations designed under this framework deliver artifact-free results that are consistent with those of classical intensity-based geometric image transformations.

Index Terms— AM-FM image models, geometric transformations, image filters, modulation domain filtering.

1. INTRODUCTION

AM-FM image models were introduced in [1] and systematically developed in [2, 3] and elsewhere. Such models seek to represent a continuous domain image $f : \mathbb{R}^2 \to \mathbb{R}$ as a sum of nonstationary components according to

$$f(\mathbf{x}) = \sum_{k=1}^{K} f_k(\mathbf{x}) \equiv \sum_{k=1}^{K} a_k(\mathbf{x}) \cos[\psi_k(\mathbf{x})], \tag{1}$$

where each component $f_k(\mathbf{x})$ is characterized in the modulation domain by a smoothly varying, positive semidefinite amplitude modulation (AM) function $a_k(\mathbf{x})$ that captures local contrast and a smoothly varying frequency modulation (FM) function $\nabla\psi_k(\mathbf{x})$ that captures the orientation and granularity of local surface patterns. The main idea is that the modulation domain representation $\{a_k, \nabla\psi_k\}_{k\in[1,K]}$ is more naturally related to human visual perception than a standard Fourier representation [1, 2] and can therefore facilitate powerful, perceptually motivated processing and analysis. Such models have been used successfully in a variety of signal analysis applications including speech recognition, image segmentation, image classification, motion estimation, content-based retrieval, and texture inpainting [3–8]. Note that the model (1) is ill-posed on at least two levels: the decomposition into components is generally defined by an appropriate multiband filterbank [3] or iterative regression [6], while the problem of uniquely defining the AM and FM functions is typically disambiguated by associating an imaginary part with each f_k, either implicitly via, *e.g.*, the multidimensional Teager-Kaiser operator [9], or explicitly using an appropriate Hilbert transform [3, 6].

For 15 years following the publication of [1], practical use of the model (1) was limited to analysis-only applications for two main reasons. First, virtually all modern applications are concerned with digital images defined on a discrete lattice; the approximation errors inherent in estimating the spatial derivatives $\nabla\psi_k$ from discrete image samples precluded the possibility of accurate AM-FM image synthesis. Second, a sufficiently jointly spatio-spectrally localized perfect reconstruction filterbank was not available to permit perfect reconstruction from the AM-FM model, even in the absence of any modulation domain processing.

These problems were addressed in [10–12] where a perfect reconstruction steerable pyramid filterbank with joint localization properties similar to the Gabor filters was used to decompose a discrete image into components and the discrete components $f_k(\mathbf{n})$ were interpolated with cubic tensor product splines which could be differentiated analytically to obtain the FM functions $\nabla\psi_k(\mathbf{n})$ on the lattice $\mathbf{n} \in \mathbb{Z}^2$. Perfect reconstruction of digital images from the model (1) was demonstrated with this approach, as well as AM-based processing including frequency selective attenuation and elementary FM processing. However, due to the phase congruence problem which we will discuss in Section 2, the modulation domain image filtering and synthesis techniques introduced in [11, 12] cannot accommodate more sophisticated processing including geometric transformations where interpolation to a new sampling lattice is required.

In this paper we address the phase congruence problem by factoring the phase congruence term out of the component FM functions to obtain a new generalized AM function and corresponding generalized FM function. This new generalized AM function resolves several phase reconstruction problems associated with AM-FM image synthesis, but fails to remain positive semidefinite. We show that this modification leads to artifact-free modulation domain filtering results. In addition, for the first time we introduce a generalized framework for modulation domain image filtering that supports sophisticated AM and FM filtering including image synthesis on transformed sampling lattices. This permits an elegant and direct extension of the modulation domain image processing theory to include important classical geometric transformations such as rotation, scaling, and non-integer translation.

2. GENERALIZED AM AND THE PHASE CONGRUENCE PROBLEM

Consider a discrete image $f(\mathbf{n}) : \mathbb{Z}^2 \to \mathbb{R}$ with respect to the model (1). For the modulation domain filtering techniques given in [11, 12], initial frequency samples $\nabla\psi_k(\mathbf{n})$ are obtained by fitting the image with a cubic tensor product spline, applying the continuous frequency demodulation algorithm given in [3], and spatially sampling the result. The phase unwrapping technique given in [13] is then applied to integrate $\nabla\psi_k(\mathbf{n})$ in a least squares (LS) sense and

This work was supported in part by the U.S. Army Research Laboratory and the U.S. Army Research Office under grant W911NF-08-1-0293.

obtain a discrete unwrapped phase function $\varphi_k(\mathbf{n})$. Because of the ambiguity inherent in the LS phase unwrapping problem, the computed phase $\varphi_k(\mathbf{n})$ is generally inconsistent with the principle phase values $\arccos[f_k(\mathbf{n})/a_k(\mathbf{n})]$ obtained from the original image components at some pixels. The solution given in [10] is to define the phase function $\psi_k(\mathbf{n})$ according to

$$\psi_k(\mathbf{n}) = \varphi_k(\mathbf{n}) + \rho_k(\mathbf{n}), \tag{2}$$

where the phase congruence term $\rho_k(\mathbf{n})$ is chosen to enforce agreement between the principle values of the LS unwrapped phase $\varphi_k(\mathbf{n})$ and the principle values of $\psi_k(\mathbf{n})$.

The phase model (2) is generally satisfactory for performing image synthesis on the discrete lattice $\mathbb{Z}^2$ – even after AM-based image filtering or elementary FM-based processing have been applied. However, the phase congruence term ρ_k generally fails to be smooth and, consequently, the presence of $\rho_k(\mathbf{n})$ in (2) tends to introduce undesirable artifacts in the reconstructed image when sophisticated FM filtering or geometric transformations requiring interpolation to a new spatial sampling lattice are applied. These artifacts arise because the integrated phase $\psi_k(\mathbf{n})$ contains jumps that are introduced to the phase by the phase congruence term $\rho_k(\mathbf{n})$. These discontinuities subsequently generate artifacts in the filtered output [12].

Here, we ameliorate the phase congruence problem by factoring $\rho_k(\mathbf{n})$ out of each term in (1) to define new generalized AM functions $A_{1k}(\mathbf{n})$ and $A_{2k}(\mathbf{n})$ through

$$\begin{aligned} f_k(\mathbf{n}) &= a_k(\mathbf{n})\cos[\psi_k(\mathbf{n})] = a_k(\mathbf{n})\cos[\varphi_k(\mathbf{n}) + \rho_k(\mathbf{n})] \\ &= a_k(\mathbf{n})\cos[\rho_k(\mathbf{n})]\cos[\varphi_k(\mathbf{n})] \\ &\quad -a_k(\mathbf{n})\sin[\rho_k(\mathbf{n})]\sin[\varphi_k(\mathbf{n})] \\ &\equiv A_{1k}(\mathbf{n})\cos[\varphi_k(\mathbf{n})] + A_{2k}(\mathbf{n})\sin[\varphi_k(\mathbf{n})]. \end{aligned} \tag{3}$$

In order to define modulation domain signal processing operations capable of delivering filtered images that are free from undesirable phase reconstruction artifacts, AM-only processing should be applied to the (non-generalized) amplitude modulation functions $a_k(\mathbf{n})$. However, for joint AM-FM filtering, the generalized AM functions $A_{1,k}(\mathbf{n})$ and $A_{2,k}(\mathbf{n})$ should be processed. FM processing should be applied only to the generalized FM functions $\nabla\varphi_k(\mathbf{n})$ and *not* to $\nabla\psi_k(\mathbf{n})$. Subsequent to such processing, the generalized AM and FM functions can be interpolated to synthesize image samples on a modified sampling lattice as required to implement geometric image transformations.

3. MODULATION DOMAIN IMPLEMENTATION OF GEOMETRIC TRANSFORMATIONS

We define three basic artifact free classical image transformations, *i.e.*, scaling, rotation, and translation in the modulation domain. Let

$$\mathcal{O}_\alpha = \begin{bmatrix} \cos(\alpha) & \sin(\alpha) \\ -\sin(\alpha) & \cos(\alpha) \end{bmatrix} \tag{4}$$

be the rotation matrix by an arbitrary angle α and let $\mathcal{R}_\alpha$ be the rotation operation by an angle α acting on the pixel lattice. Let $\nabla\varphi_k(\mathbf{n}) = [U_k(\mathbf{n})\ V_k(\mathbf{n})]^T$ be the gradient of the phase $\varphi_k(\mathbf{n})$, where $U_k(\mathbf{n})$ and $V_k(\mathbf{n})$ are the horizontal and vertical components of the gradient, respectively. Let $\hat{A}_{ik}$ be the generalized AM, $i = 1, 2$ as in (3), and let $\nabla\hat{\varphi}_k(\mathbf{n})$ be the generalized FM functions. Since the image is described by a sum of K AM-FM components in the model (1), the final synthesized output image $\hat{f}(\mathbf{n})$ after transformation is given by a linear sum of filtered components $\hat{f}(\mathbf{n}) = \sum_{k=1}^{K} \hat{f}_k(\mathbf{n})$ in which the same transformation is applied to all K components in parallel.

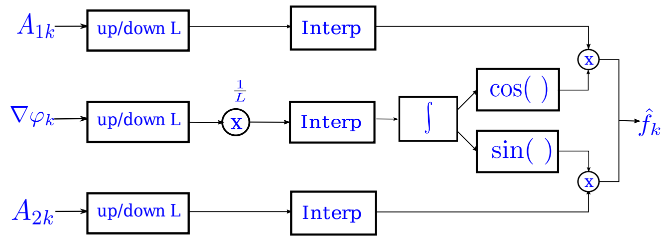

Fig. 1. Block diagram of modulation domain image scaling.

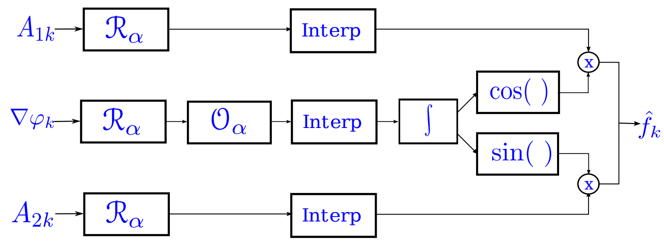

Fig. 2. Block diagram of modulation domain image rotation.

3.1. Scaling

The modulation domain scaling operation is designed to admit integer, rational, and general irrational scaling factors. For example, if we enlarge the image by two, the magnitude of the FM field of the enlarged image must be decreased by two. Consequently, to produce a modulation domain image magnification operation that is consistent with classical image scaling, we design a filtering scheme to accommodate for these changes of the gradient field $\varphi_k(\mathbf{n})$.

The modulation domain scaling operation is depicted in Fig. 1. The AM signals $A_{ik}(\mathbf{n})$ are first up/down sample by a predefined (non-integer) factor L and then are interpolated by either bilinear or bicubic interpolants. The FM signal $\nabla\varphi_k(\mathbf{n})$ is also up/down sample by the predefined factor L. This modified gradient signal is then compensated by $1/L$ in order to preserve the texture structure spacing and orientations. The modified gradient is then integrated to find the modified phase function $\hat{\varphi}_k(\mathbf{n})$. As the processed gradient field $\hat{\varphi}_k(\mathbf{n})$ may not be conservative, the modified phase is computed by performing the least square phase unwrapping method proposed by Ghiglia and Romero [13]. The scaled output signal is then given as a summation of the filtered components $\hat{f}_k(\mathbf{n})$.

3.2. Rotation

A classical image rotation involves a rotation of the image grid and an interpolation scheme. In the modulation domain, a rotation on the image grid will also rotate the orientation of the gradient field $\nabla\varphi_k(\mathbf{n})$. In order to preserve the visually important texture structure and orientation, we implement the orientation change of the gradient field by multiplying with a rotation matrix $\mathcal{O}_\alpha$.

The modulation domain image rotation operation is described in Fig. 2. The rotation operator $\mathcal{R}_\alpha$ is first applied to the AM signals $A_{ik}(\mathbf{n})$. The rotated AM signals are then interpolated to find values lying on the pixel lattice. The rotation operator $\mathcal{R}_\alpha$ is also applied to the gradient field $\nabla\varphi_k(\mathbf{n})$ and then multiplied with the rotation matrix $\mathcal{O}_\alpha$. Therefore, the rotation operation for the FM signal $\nabla\varphi_k(\mathbf{n})$ is defined as $\mathcal{R}_\alpha\mathcal{O}_\alpha\nabla\varphi_k(\mathbf{n})$. Similar to Section 3.1, the modified gradient field $\nabla\hat{\varphi}_k$ is then integrated to find the modified phase $\hat{\varphi}_k$ by solving for the least square solution of the phase unwrapping problem. Finally, the rotated output image is computed as a linear sum of the rotated components $\hat{f}_k(\mathbf{n})$.

In addition, for the rotation of the FM field it may be shown that the counter rotation operator $\mathcal{O}_\alpha$ commutes with the lattice rotation operator $\mathcal{R}_\alpha$:

Theorem: $\mathcal{R}_\alpha \mathcal{O}_\alpha \nabla \varphi_k(\mathbf{n}) = \mathcal{O}_\alpha \mathcal{R}_\alpha \nabla \varphi_k(\mathbf{n})$.

Proof: straightforward, but omitted for brevity.

3.3. Translation

Since we model $f(\mathbf{n}) = \sum_{k=1}^{N} a_k(\mathbf{n}) \cos[\psi_k(\mathbf{n})]$, the translated output by displacement vector $\mathbf{u} = (u_0, v_0)$ is given by

$$f(\mathbf{n}-\mathbf{u}) = \sum_{k=1}^{N} a_k(\mathbf{n}-\mathbf{u}) \cos[\psi_k(\mathbf{n}-\mathbf{u})], \tag{5}$$

where $\mathbf{u} \in \mathbb{R}^2$. Therefore, the modulation domain translation operation can be achieved by translating $a_k(\mathbf{n})$ and $\psi_k(\mathbf{n})$ by $\mathbf{u}$, which generally yields samples that fail to lie on the discrete sampling lattice. We then apply bicubic interpolation to the resulting generalized AM and FM functions to synthesize new image samples on the translated sampling lattice.

4. RESULTS AND DISCUSSION

We perform two classical image transformation operations, *e.g.*, scaling and rotation with both natural images and familiar texture test images. We use a bicubic interpolation scheme for both spatial transformation and modulation domain transformation. The results are shown in Fig. 3. The first row shows results of upsampling the Boat and Barbara images by a factor of 2.0. The second row depicts the results of rotating the Boat and Reptile images clockwise by $25°$. The first and the third columns are pixel domain image scaling and rotation results, while the second and fourth columns show the results of these operations performed in the modulation domain.

Perceptually, the results given by the modulation domain processing are consistent with those obtained via pixel domain processing. For the upsampling example of Barbara, the modulation domain technique in Fig. 3(d) can preserve the diagonal stripes in Barbara's tie while the classical interpolation technique in Fig. 3(c) fails to retain accurate texture orientations. The rotation results given in Fig. 3(e)-(h) show that the techniques proposed in this paper are effective for extending the modulation domain filtering theory to deliver geometric transformation results comparable in fidelity to those obtained by traditional pixel domain image processing methods.

The quantitative comparison between the classical bicubic interpolation and our proposed algorithm is shown in Table 1. We restrict the comparison to the upsampling operation because of the lack of ground truth data for the rotation and translation operations. We measure the performance in terms of the peak signal to noise ratio measure (PSNR) and the structural similarity index (SSIM) index [14]. For the upsampling operation, the PSNR performance of the proposed algorithm is worse than that of the classical bicubic interpolation. The proposed algorithm, however, outperforms the classical bicubic interpolation in the perceptually motivated image quality measure SSIM. While the PSNR is a popular quality measure in the literature, it has been proven to be a unreliable metric in many image processing applications [15]. Furthermore, our goal in this paper is not to argue that the proposed algorithms perform better than the classical interpolation algorithms. Rather, we aim to achieve comparable image transformation results but using modulation domain processing as opposed to pixel domain processing.

Table 1. Comparison of the upsampling operation.

	PSNR (dB)		SSIM	
	Bicubic	AM-FM	Bicubic	AM-FM
Boat	**25.645**	25.314	0.765	**0.790**
Barbara	**32.881**	32.482	0.704	**0.729**

5. CONCLUSION

We proposed a generalized framework to perform image transformations in the modulation domain. The modulation domain geometric image transformation results obtained by the proposed approach are visually consistent with those obtained by traditional pixel domain techniques. In the upsampling case, we showed quantitatively that the modulation domain technique can perform better than traditional spatial interpolation techniques with respect to the SSIM figure of merit. For future work, we will study quantitatively the signal processing gain of modulation domain techniques and expand this generalized theory to other nonlinear image processing operations.

6. REFERENCES

[1] A. C. Bovik, M. Clark, and W. S. Geisler, "Multichannel texture analysis using localized spatial filters," *IEEE Trans. Pattern Anal. Machine Intell.*, vol. 12, no. 1, pp. 55–73, Jan. 1990.

[2] A. C. Bovik, N. Gopal, T. Emmoth, and A. Restrepo, "Localized measurement of emergent image frequencies by Gabor wavelets," *IEEE Trans. Info. Theory*, vol. 38, no. 2, pp. 691–712, Mar. 1992.

[3] J. P. Havlicek, D. S. Harding, and A. C. Bovik, "Multidimensional quasi-eigenfunction approximations and multicomponent AM-FM models," *IEEE Trans. Image Proc.*, vol. 9, no. 2, pp. 227–242, Feb. 2000.

[4] P. Maragos, J. F. Kaiser, and T. F. Quatieri, "Energy separation in signal modulations with applications to speech analysis," *IEEE Trans. Signal Proc.*, vol. 41, no. 10, pp. 3024–3051, Oct. 1993.

[5] K. Langley, D. J. Fleet, and T. J. Atherton, "Multiple motions from intantaneous frequency," in *Proc. Int'l. Conf. Comput. Vision and Pattern Recog.*, Champaign, IL, Jun. 15-18, 1992, pp. 846–849.

[6] N. E. Huang, Z. Shen, S. R. Long, M. C. Wu, H. H. Shih, Q. Zheng, N. -C. Yen, C. C. Tung, and H. H. Liu, "The empirical mode decomposition and the Hilbert spectrum for nonlinear and non-stationary time series analysis," *Proc. R. Soc. Lond. A*, vol. 454, pp. 903–995, 1998.

[7] S. T. Acton, D. P. Mukherjee, J. P. Havlicek, and A. C. Bovik, "Oriented texture completion by AM-FM reaction-diffusion," *IEEE Trans. Image Proc.*, vol. 10, no. 6, pp. 885–896, Jun. 2001.

[8] M.S. Pattichis and A.C. Bovik, "Analyzing image structure by multidimensional frequency modulation," *IEEE Trans. Pattern Anal., Machine Intel.*, vol. 29, no. 5, pp. 753–766, May 2007.

[9] P. Maragos and A. C. Bovik, "Image demodulation using multidimensional energy separation," *J. Opt. Soc. Amer. A*, vol. 12, no. 9, pp. 1867–1876, Sep. 1995.

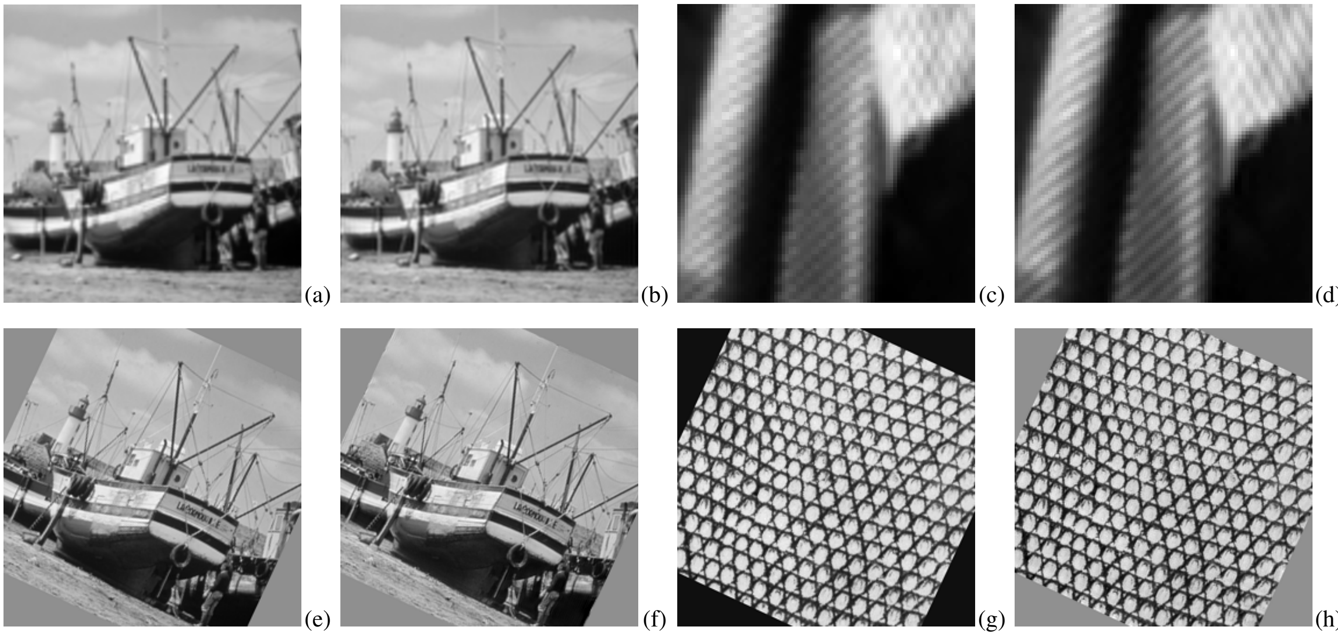

Fig. 3. Examples. (a) Boat: Upsampled by 2.0 by bicubic interpolation. (b) Boat: Upsampled by 2.0 in modulation domain. (c) Barbara: Upsampled by 2.0 by bicubic interpolation. (d) Barbara: Upsampled by 2.0 in modulation domain. (e) Boat: Rotated by 25° clockwise using bicubic interpolation. (f) Boat: Rotated by 25° clockwise in modulation domain. (g) Reptile: Rotated by 25° clockwise using bicubic interpolation. (h) Reptile: Rotated by 25° clockwise in modulation domain.

[10] R. A. Sivley and J. P. Havlicek, "Perfect reconstruction AM-FM image models," in *Proc. IEEE Int'l. Conf. Image Proc.*, Atlanta, GA, Oct. 8-11, 2006, pp. 2125–2128.

[11] C. T. Nguyen and J. P. Havlicek, "AM-FM image filters," in *Proc. IEEE Int'l. Conf. Image Proc.*, San Diego, CA, Oct. 12-15, 2008, pp. 789–792.

[12] C. T. Nguyen, P.A. Campbell, and J. P. Havlicek, "FM filters for modulation domain image processing," in *Proc. IEEE Int'l. Conf. Image Proc.*, Cairo, Egypt, Nov. 7-11, 2009, pp. 3973–3976.

[13] D. C. Ghiglia and L. A. Romero, "Robust two-dimensional weighted and unweighted phase unwrapping that uses fast transforms and iterative methods," *J. Opt. Soc. Amer. A*, vol. 11, no. 1, pp. 107–117, Jan. 1994.

[14] Z. Wang, A. C. Bovik, H. R. Sheikh, and E. P. Simoncelli, "Image quality assessment: From error visibility to structural similarity," *IEEE Trans. Image Proc.*, vol. 13, no. 4, pp. 600–612, Apr. 2004.

[15] Z. Wang and A. C. Bovik, "Mean squared error: love it or leave it? - a new look at signal fidelity measures,," *IEEE Signal Proc. Magazine*, vol. 26, no. 1, pp. 98–117, Jan. 2009.